Electrochimica Acta 243 (2017) 90–97

Contents lists available at ScienceDirect

Electrochimica Acta

journal homepage: www.elsevier.com/locate/electacta

Electrochemical production of colloidal sulphur by oxidation of sulphide ion at lead coated-2- and -3-dimensional rotating cylinder anode surfaces

J.P. Fornés, J.M. Bisang*

Universidad Nacional del Litoral, CONICET, Programa de Electroquímica Aplicada e Ingeniería Electroquímica (PRELINE), Facultad de Ingeniería Química, Santiago del Estero 2829, S3000AOM Santa Fe, Argentina

ARTICLE INFO

Article history:
Received 13 March 2017
Received in revised form 8 May 2017
Accepted 8 May 2017
Available online 10 May 2017

Keywords:
colloidal sulphur
hydrogen sulphide
electrochemical reactor
sulphur production

ABSTRACT

An electrochemical reactor with a rotating cylinder electrode is analysed for the production of colloidal sulphur by oxidation of sulphide ions with a concentration of 2 g dm^{-3} in alkaline solutions at 80 °C. The anode, coated with lead, was either a smooth cylinder or a three-dimensional one. The formation of polysulphides takes place in a wide range of potential of 0 to 1.2 V, against saturated calomel electrode (SCE), at a constant current density, which is independent on the rotation speed for values higher than 100 rpm. For the smooth anode the space time yield was 0.4 kg m^{-3} h^{-1}. However, this parameter was increased 5 times in the potential range of 0.8 V to 1.2 V, vs. SCE, by using a three-dimensional structure with a bed depth of 8 mm. The specific energy consumption was 11.7 kW h kg^{-1} with a current efficiency near 100%. When the sulphide ions were replenished by dissolution of hydrogen sulphide from a gas stream a further increase of the space time yield to 3.6 kg m^{-3} h^{-1} was achieved. At the end of the experiments the solution was acidified forming colloidal sulphur particles of different shapes with an average size of 5 μm.

1. Introduction

Hydrogen sulphide is produced in several industrial and domestic processes. This contaminant generates environmental issues, corrosion problems and degradation of materials requiring its removal from effluents and the recovery of their constituents becomes very attractive. Thus, Zaman and Chakma [1] reviewed the possibilities and limitations of thermal, thermochemical, electrochemical, photochemical and plasmochemical technologies for the production of hydrogen and sulphur from hydrogen sulphide. However, none of these methods are used today. From the industrial point of view, the Claus process [2] is applied for the deletion of hydrogen sulphide from fuels allowing only the recuperation of sulphur and steam from the heat of reaction. This procedure is economically feasible at very large plants and it presents as disadvantage that hydrogen is inconsiderate. An improved alternative is its replacement by an electrochemical method. Recently, Kelsall [3] summarised the electrochemical process options for the removal of hydrogen sulphide. Despite this proposal is very old [4], the main drawback is the anode passivation due to the electrode surface is cover by insulated sulphur. This adverse effect causes a decay of the current over time and to overcome this problem different strategies have been proposed:

- Change of the electrode material in order to avoid the sulphur generation and to promote the formation of soluble oxyanions of sulphur. Thus, Rajalo et al. studied the electrochemical oxidation of sulphide, mainly to sulphate, from tannery wastewaters by using either a parallel-plate reactor [5] or a modified hydrocyclone cell [6] with a titanium-manganese dioxide anode. Waterston et al. [7] examined the use of a boron-doped diamond anode for the conversion of sulphide to sulphate with current efficiency of 90%. However, this approach requires the transference of 8 electrons increasing the specific energy consumption in comparison with the oxidation to sulphur.
- Production of polysulphides by using a strong alkaline anolyte. Behm and Simonsson reported on this strategy with platinum [8], a mixed iridium-tantalum oxide coated titanium [9], nickel [10] or graphite [11] as anode materials applied to the white liquor for the pulp and paper industry. An interesting alternative of this concept is achieved by a carefully control of pH and temperature of the electrolyte, requiring a sequence of three

* Corresponding author.
E-mail address: jbisang@fiq.unl.edu.ar (J.M. Bisang).

http://dx.doi.org/10.1016/j.electacta.2017.05.050
0013-4686/

different units: a scrubber, a neutralization tank and a divided electrochemical reactor. Thus, all unwanted side reactions are eliminated, sulphide or bisulphide are oxidised to polysulphides at the anode and sulphur precipitation takes place in the bulk solution or near the electrode surface [12,13]. Based on this experience, Petrov and Srinivasan [14] proposed a new schema of the above process with sulphur precipitation out of the electrochemical reactor. Likewise, the aqueous sulphide/polysulphide redox couple is also attractive for energy conversion and storage applications [15–17].

- The increase of temperature at values higher than 60 °C eliminates the blocking of the electrode surface [18], giving a practical method to circumvent the problem.
- Use of an organic solvent for the extraction of the sulphur anodically formed. Shih and Lee [19] reported the use of a continuous stirred tank electrochemical reactor with platinum as electrodes fed with an emulsion of toluene in a basic, 5 M NaOH, sulphide, 0.1 M, solution. The volume ratio between the organic and aqueous phases was 1:5. The sulphur-containing toluene solution, separated by decantation, was evaporated to generate sulphur powder. A high value of the cell potential difference is reported, ranging from 1.8 to 4.8 V, due to the high resistance of the emulsion.
- Use of surfactants. Qing-feng et al. [20] reported that sulphur is loosely adhered to the graphite electrode surface when HTAB, hexadecyltrimethylammonium bromide, is added to the anolyte.
- Cathodic dissolution of the sulphur anodically deposited. Dutta et al. [21] proposed the switching of the electrodes alternately as anode or cathode. During the anodic cycle sulphur cover the electrode surface and the electrodeposited sulphur is reduced to sulphide/polysulphides during the cathodic cycle. Sulphur can be recuperated as a solid product either by adjusting the pH to near neutral or lightly aerating the solution.
- Application of pulse current supply. Lu *et al.* [22] showed that a pulsed electrochemical process is a promising method for efficient and sustainable sulphide removal from sewage, indicating that the anodic passivation is inhibited.
- Continuous reactivation of the anode surface by mechanically moving a cylindrical rotating electrode through different potential regions. Farooque and Fahidy [23] proposed a reactor with a rotating anode between three wiper blades forming three separate compartments. In the first one, sulphur is formed by oxidation of sulphide; in the second the anode surface is washed with piperidine and in the last compartment the anode is rinsed with deionised water.
- Use of indirect electrochemistry. Hydrogen sulphide is oxidised to sulphur by using an oxidising agent which is regenerated at the anode of an electrochemical reactor. Kalina and Maas analysed the employ of iodine in acid media [24] or iodate in alkaline solutions [25]. Chandrasekara Pillai *et al.* [26] studied the oxidative removal of hydrogen sulphide be means of the redox mediator Ce(IV)/Ce(III).

The spontaneous electrochemical removal of sulphide was studied by Dutta et al. [27] by using a lab scale fuel cell with the reduction of ferricyanide as cathodic reaction. Elemental sulphur was the primary final anodic product. Its deposition on the anode appeared to limit the operation of the equipment after three months of testing, requiring periodic removal of the accumulated sulphur from the electrode. The development of sustainable solutions to take out the precipitate is recognised as necessary for the application of the procedure.

The feasibility of electrochemical concentration for removal of hydrogen sulphide in a molten electrolyte with porous carbon electrodes was examined by Lim and Winnick [28]. Coal gas containing hydrogen sulphide is fed to the cathodic chamber of an electrochemical cell. Hydrogen evolution takes place at the cathode, sulphide ions migrate to the anode giving elemental sulphur vapour, which is converted to hydrogen sulphide by the introduction of hydrogen.

The electrochemical removal of hydrogen sulphide from polluted brines was analysed by Ateya et al. by using either planar [29] or porous flow through electrodes [30]. In both cases the feasibility of the process was demonstrated and the passivation of the anode is again recognised as the main difficulty of the procedure.

The rotating cylinder electrode presents turbulent flow conditions at moderate rotation rates achieving good mass-transfer characteristics, being the current and potential distributions substantially uniform and being it also possible to operate the system with a superimposed axial flow, which does not usually modify mass-transfer behaviour. This reactor shows widespread acceptance in a number of interdisciplinary fields and its versatility has been fully demonstrated [31–33].

Despite of the aforementioned works revealing an intensive research, the subject must be still considered in order to overcome the problem of anode passivation. Thus, the aim of the present contribution is to analyse an affordable electrochemical reactor to produce elemental sulphur by oxidation of hydrogen sulphide. The impact of temperature and pH on sulphide removal is also investigated. In addition, the performance of the reactor is evaluated to further the application potential of the process.

2. Experimental

2.1. Rotating disc electrode experiments

The criteria for the selection of the anode material were corrosion resistance, selectivity toward the formation of sulphur and stability in an alkaline solution. Between the proposed materials, gold [34] and platinum [8] are so expensive that their use in a full-scale cell is not feasible. Nickel presents good activity for sulphide oxidation, but can be deactivated by the formation of a nickel oxide/sulphide surface layer [10] and also shows some evidence of corrosion at high anodic potentials [15]. Graphite is recognised as a promising anode material due to the low cost and good catalytic properties [11]. Scharifker et al. [35] reported on the electrodeposition of lead sulphide from a sulphide solution on a lead anode but the oxidation of sulphide was not studied at this material. Thus, graphite, nickel and lead were examined to verify its properties working as anode for the oxidation of sulphide.

The working electrode was a rotating disc made of graphite or lead, 4 mm in diameter, and nickel, 3 mm in diameter, embedded in a Teflon cylinder of 10 mm diameter. As counter electrode a platinum wire, 1 mm diameter and 100 mm long, was used. A saturated calomel electrode was employed as reference and the potentials are referred to this electrode. The surface of the working electrode was polished to a bright mirror finish with slurry of 0.3 μm alumina powder and it was washed with distilled water. The experiments were performed, at different temperatures, under a slow potentiodynamic sweep of 2 mV s^{-1} in order to come close to steady-state polarization curves.

2.2. Rotating cylinder electrode experiments

The experiments were performed in a batch reactor, 95 mm internal diameter and 140 mm high. The reactor was thermostated by a heating jacket. Fig. 1, part (a), depicts the experimental arrangement. The working electrode was formed by a copper cylinder coated with lead, 41 mm diameter and 91 mm long. Lead was electroplated on the copper cylinder at a current density of 17 mA cm^{-2} during 64 h using a fluoborate bath [36] to obtain a

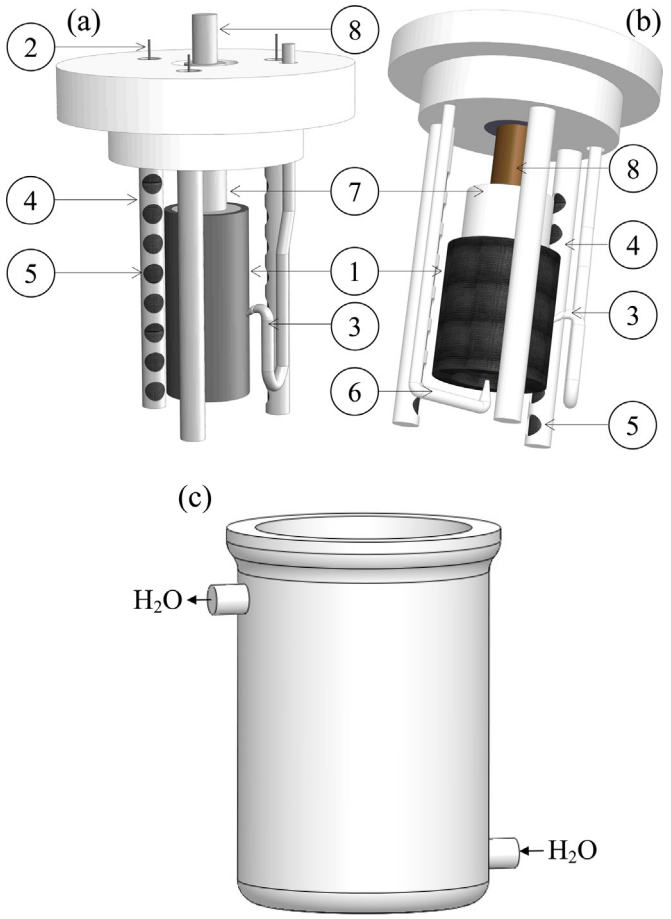

Fig. 1. Schematic representation of the electrochemical reactor. (a) Arrangement with a smooth rotating cylinder electrode. (b) Arrangement with a three-dimensional rotating cylinder electrode. (c) Glass vessel. (1) Working electrode; (2) counter electrode; (3) Luggin capillary; (4) cathodic compartments; (5) windows for the cathodic exchange membrane; (6) gas feeder; (7) Teflon sleeve; (8) electrode shaft.

coating of high purity, 99.99% [37]. After electroplating, the electrode was turned to give a straight cylinder and its surface was polished with emery paper 2500. The final lead thickness was 1.5 mm. As cathode were used three platinum wires, 1 mm diameter and 120 mm long. Each cathode was separated from the anodic compartment by a cationic exchange membrane, Nafion® 966, inserted between two perforated Teflon tubes, giving three cathodic compartments, 13.5 mm external diameter, and placed symmetrically around the rotating electrode. The gap between the rotating cylinder and the cationic exchange membrane was 13 mm. The working electrode and the counter electrode were concentric. As reference a saturated calomel electrode was used connected to a Luggin capillary located in the mid-region of the rotating electrode. The upper end of the rotating electrode was attached to the motor shaft.

2.3. Three-dimensional rotating cylinder electrode experiments

The reactor and the counter electrode were the same as above. The working electrode was a three-dimensional rotating cylinder anode, 35 mm internal diameter, 52 mm height with different electrode thicknesses. Fig. 1, part (b), shows schematically the anode, which was made by winding a 304 stainless steel woven-wire screen, 8 mesh size, (0.7 mm wire diameter and 2.48 mm distance between wires). The surface area per unit electrode volume, A_s, was 1228 m^{-1} with a void fraction, ε, of 0.8, which were calculated by using the following equations [38]

$$A_s = \frac{4w}{d\delta V_e} \quad (1)$$

and

$$\varepsilon = 1 - \frac{w}{\delta V_e} \quad (2)$$

where w is the weight of the electrode, d is the wire diameter, V_e the volume of the three-dimensional structure and δ is the density of the electrode material. The stainless steel three-dimensional structure was plated with lead using a fluoborate bath [36]. Three electrode thicknesses were investigated (5.3 mm, 8 mm and 11 mm). The mean value of the lead thickness was approximately 0.28 mm, giving a surface area per unit electrode volume of the lead-coated three-dimensional structure of 1766 m^{-1} with a void fraction of 0.55. The ratio between the surface areas of the three-dimensional structures to that of the smooth rotating cylinder electrode was 5, 10 and 13 for the bed depths of 5.3, 8 and 11 mm, respectively. A perforated Teflon disc, centrally positioned, was employed as a support of the three-dimensional electrode. Three lead-plated bolts passed through the bed thickness, pressing the rotation axis and thus ensuring electric contact. The lower part of the three-dimensional electrode was open but the upper part was joined to a Teflon sleeve in order to orientate the electrolyte flow, produced by the rotation of the electrode, through the sheet pack. A saturated calomel electrode was used as reference connected to a Luggin capillary positioned at the mid-region of the outer face of the three-dimensional anode. Some experiments were performed introducing at the bottom of the anode a gas phase with 5% of H_2S in nitrogen. In this case the rotation of the electrode promotes a simultaneous co-current radial flow of the liquid and gas phases through the three-dimensional structure.

2.4. Electrolyte preparation and experimental procedures

Two types of electrolyte were employed. In the single-phase experiments it was used a solution with a sulphide concentration of 2 g dm^{-3} at pH 10, prepared with sodium sulphide nonahydrate and adjusting the pH with the addition of sulphuric acid. In the biphasic experiments, gas/liquid, a mix of 5% H_2S and 95% N_2 was bubbled at 0.1 MPa into the solution of sulphide, without adjusting of pH, via a gas distributor placed at the lower end of the rotating three-dimensional electrode. The gas volumetric flow rate was 8×10^{-6} $m^3 s^{-1}$ under ambient conditions. Thus, the anodic reaction is

$$n\ HS^- + n\ HO^- \rightarrow S_n^{2-} + n\ H_2O + (2n-2)\ e^- \quad (3)$$

and at the cathode takes place hydrogen evolution

$$2\ H_2O + 2\ e^- \rightarrow H_2 + 2\ HO^- \quad (4)$$

An electrochemical divided reactor is necessary to avoid the reduction at the cathode of polysulphides formed at the anode. Likewise, the level of the electrolyte coincides with the upper part of the Teflon sleeve in order to minimise the air inlet due to the vortex produced by the rotation of the electrode. Thus, the oxidation of polysulphides by oxygen [39] was avoided.

The initial concentration of sulphide was measured iodometrically. Thus, sulphide is reacted with an excess of iodine in acid solution, and the remaining iodine is then determined by titration with sodium thiosulphate, using starch as an indicator [40]. At the end of the experiment the pH of the solution

was adjusted to a value near 1 to form colloidal sulphur according to

$$S_n^{2-} + H^+ \rightarrow (n-1)\ S\ +\ HS^- \quad (5)$$

Sulphur was left to decant, the solution was taken out and the amount of elemental sulphur, m, in the precipitate was determined with the method described by Morris et al. [41]. Thus, sulphur was oxidised to thiosulphate by boiling in a sodium sulphite solution, the excess of sulphite was bound with formaldehyde and the thiosulphate was determined by iodometric titration.

The experiments were performed potentiostatically with a solution volume of 0.75 dm^3. Both, cell potential difference, U, and current, I, were measured. From the above measurements, the mean values of the current efficiency, β, the specific energy consumption, E_s, and the space time yield, ρ, were calculated with the following equations:

$$\beta = \frac{2Fm(t_f)}{M\int_0^{t_f} I(t)dt} \quad (6)$$

$$E_s = \frac{\int_0^{t_f} I(t)U(t)dt}{m(t_f)} \quad (7)$$

and

$$\rho = \frac{m(t_f)}{Vt_f} \quad (8)$$

where M is the molar mass of sulphur, t is the time, t_f is the duration of the experiment and V is the solution volume in the reactor.

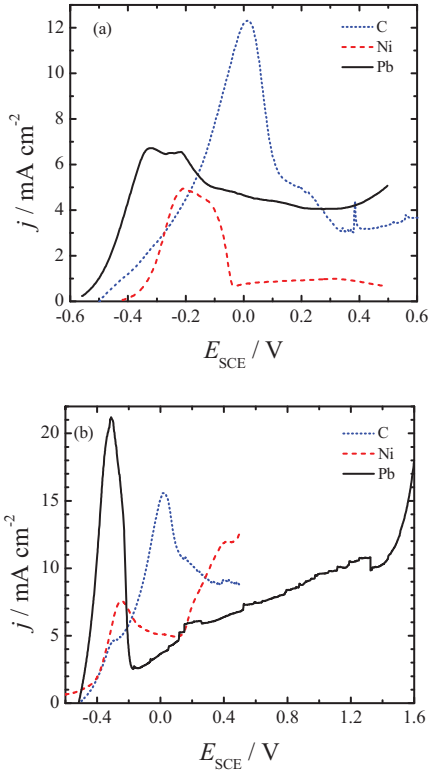

Fig. 2. Polarization curves for sulphide oxidation at rotating disc electrodes of graphite, nickel and lead. Electrolyte: 2 g $S^=$ dm^{-3}, pH 10. (a): T = 50 °C. (b): T = 80 °C. ω = 1000 rpm. Potential sweep rate: 2 mV s^{-1}.

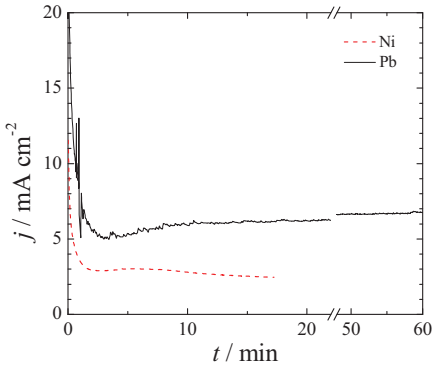

Fig. 3. Current density as a function of time for sulphide oxidation at rotating disc electrodes of nickel and lead. Electrolyte: 2 g $S^=$ dm^{-3}, pH 10. E_{SCE} = −0.25 V. T = 80 °C. ω = 1000 rpm.

3. Results and discussion

3.1. Preliminary studies with rotating disc electrodes

Fig. 2 shows typical polarization curves at two temperatures. It can be observed that the current begins at a potential near −0.6 V, which corresponds to the dielectric breakdown of the lead sulphide film [35]. A sharp increase in current is observed at higher potentials, reaching a peak because of the electrode surface area in all cases is passivated when the potential becomes more anodic. Nickel presents corrosion at potentials higher than 0.1 V. Fig. 3 reports on the current density as a function of time for nickel and lead at 80 °C, where it is corroborated the passivation of both metals. From Figs. 2 and 3 it can be concluded that the best performance as anode material is shown by lead at 80 °C.

3.2. Studies with a rotating cylinder electrode

Fig. 4 shows the current as a function of time for three independent experiments performed potentiostatically at 0.6 V, which corresponds to the mean value of the potential range to carry out the oxidation of sulphide. The full line corresponds to a smooth cylinder where the rotation speed was stepwise changed from 500 rpm to 1000 rpm with increasing step sizes of 250 rpm, whereas in the dashed line the rotation speed was decreased with a stepwise of 100 rpm. This last procedure was also applied to a three-dimensional cylinder, 5.3 mm bed thickness, represented as a dotted line. When a lead electrode is immersed in the electrolyte and also during the first stage of the experiment, the surface of the

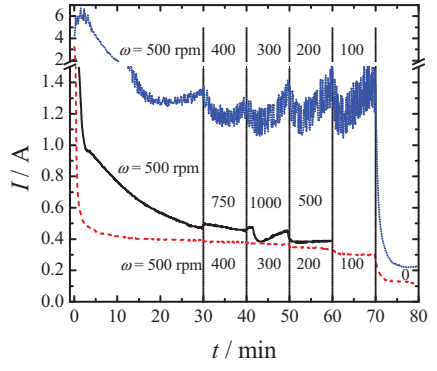

Fig. 4. Current as a function of time for sulphide oxidation at rotating cylinder electrodes coated with lead for different values of the rotation speed. Full and dashed lines: smooth electrode. Dotted line: three-dimensional electrode, 5.3 mm thickness. Electrolyte: 2 g $S^=$ dm^{-3}, pH 10. T = 80 °C. E_{SCE} = 0.6 V.

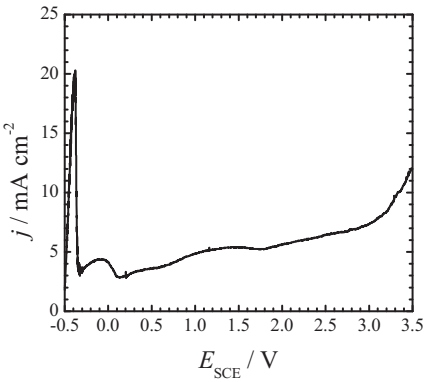

Fig. 5. Polarization curve for sulphide oxidation at a smooth rotating cylinder electrode coated with lead. Electrolyte: 2 g S$^{=}$ dm^{-3}, pH 10. Pretreatment: 30 min at E_{SCE} = 0.6 V. T = 80 °C. ω = 500 rpm. Potential sweep rate: 1 mV s^{-1}.

anode is covered by a black thin layer, poorly adherent. According to Scharifker et al. [35], it can be assumed that this layer is formed by lead sulphide, which proceeds from the reaction of HS^- ions with the lead ions from the dissolution of the anode. In Fig. 4, it can also be observed that the stationary current is independent on the rotation speed showing that the reaction rate is not influenced by mass-transfer. Only at rotation speeds lower than 100 rpm it is detected a pronounced diminution of the current density. A similar finding was reported by Rajalo and coworkers [6], who proposed that a chemical intermediate is limiting the rate of sulphide oxidation. The dotted line, corresponding to a three-dimensional electrode, shows the same behaviour as the smooth cylinder, only a higher current is observed as a consequence of the larger electrode surface area. At the end of the experiment a polarization curve at a scan rate of 1 mV s^{-1} was obtained with the smooth rotating cylinder electrode, which is shown in Fig. 5. It can be observed a wide range of potential where the oxidation of sulphide occurs with a small increase in current. A similar behaviour is detected in the polarization curve of a lead rotating disc electrode at 80 °C reported on Fig. 3, part (b). From the above experimental results, it can be stated that the rate of sulphide oxidation at a lead anode is not affected by the mixing conditions in the electrolyte around the electrode, which are very different for both rotating systems. Likewise, oxygen evolution takes place at potentials higher than 1.4 V.

Fig. 6 displays typical curves of the current as a function of time for the sulphide oxidation using the above batch reactor with a smooth rotating cylinder electrode for a rotation speed of 500 rpm at different potentials. At the start of the experiment the current shows an oscillatory behaviour, which was more marked as lower is the anodic potential, but after a few minutes the passivation of

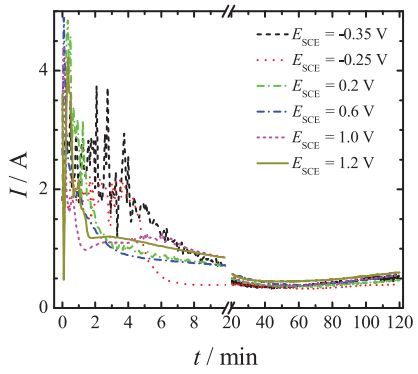

Fig. 6. Current as a function of time for sulphide oxidation at a smooth rotating cylinder electrode coated with lead at different potentials. Electrolyte: 2 g S$^{=}$ dm^{-3}, pH 10. T = 80 °C. ω = 500 rpm.

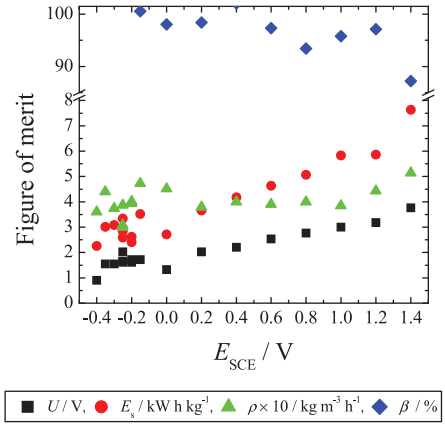

Fig. 7. Figures of merit for the colloidal sulphur production at a smooth rotating cylinder electrode coated with lead as a function of the anodic potential. Electrolyte: 2 g S$^{=}$ dm^{-3}, pH 10. T = 80 °C. ω = 500 rpm.

the anode takes place. The oscillations are presumably resulting from the formation of the passivation layer. At longer times the current approaches the same value independent on the applied potential, achieving 0.55 A, with a current density of 4.7 mA cm^{-2}. Then, the small increase in current, for lead as anode material, in the potential range of −0.2 V to 1.2 V reported on Fig. 2, part (b) and Fig. 5 is a consequence of the pseudo stationary nature of the polarization curves. At potentials higher than 1.4 V it was observed the breaking off of the black thin layer at the surface of the anode.

Fig. 7 reports on the figures of merit for the production of colloidal sulphur as a function of the anodic potential, which represent mean values for each experiment after two hours of electrolysis. The pH changes from 10 to a final value of 9. As a consequence of the oscillatory behaviour of current at the start of the experiment showed in Fig. 6 a high scattering in the results are observed at potentials more negative than −0.1 V. However at potentials higher than −0.1 V and as expected, an increase in the cell potential difference, U, and in the specific energy consumption, E_s, is observed when the anodic potential becomes more positive. The current efficiency for sulphur production, β, is higher than 95% and decreases at potentials more anodic than 1.4 V. The lost of current efficiency can be attributed to the formation of sulphur-containing species such as sulphite [12] and at the higher potentials due to oxygen evolution, as side anodic reactions. For this reason an anodic potential of 1.2 V represents a maximum value in order to avoid, according to Fig. 6, the deterioration of the electrode and to retain a high current efficiency. The space time yield, ρ, is about 0.4 kg m^{-3} h^{-1} in the potential range of 0.2 V to 1.2 V.

Considering the above figures it can be concluded that the oxidation of sulphides at a smooth lead anode takes place under a constant current density and with a high current efficiency for sulphur production in a wide range of potentials, near 1.2 V. This behaviour suggests the use of three-dimensional rotating cylinder electrodes in order to improve the reactor performance.

3.3. Studies with three-dimensional rotating cylinder electrodes

Fig. 8 shows typical curves of the current as a function of time for the sulphide oxidation with three-dimensional rotating cylinder electrodes for a rotation speed of 500 rpm at different values of the potential and the bed depth. A similar behaviour to that reported in Fig. 6 is observed with an increase in current due to the enlargement of the electrode surface area in the three-dimensional structure. Furthermore, for a given value of the bed depth the current is little dependent on the electrode potential applied to the external face of the three-dimensional structure

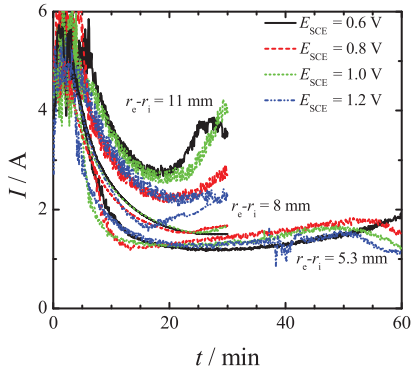

Fig. 8. Current as a function of time for sulphide oxidation at three-dimensional rotating cylinder electrodes coated with lead at different values of potential and bed depth. Electrolyte: 2 g S$^=$ dm^{-3}, pH 10. T = 80 °C. ω = 500 rpm.

revealing that the effective bed thickness is similar in all cases. In a three-dimensional electrode the surface area is not fully used because the wires of the net have a shielding effect and also, from a microscopic point of view, each wire has a current distribution which varies with position on the surface. Alkire and Gracon [42] adopted 0.81 as a multiplier of the specific surface area to obtain a good correlation between experimental and theoretical results when the test reaction was ferricyanide reduction. Bisang [38] reported 0.77 as a mean value for copper deposition as test reaction. The increase in current with the bed depth is mainly a consequence of the enlargement of the electrode surface area due to the increase of the external radius of the three-dimensional structure, despite the effective bed thickness is similar in all cases.

Assuming that all points of the three-dimensional structure are under limiting current conditions, giving a maximum space time yield, the theoretical bed depth in the direction of the current flow, $r_e - r_i$, is given by the following expression [43]:

$$\Delta E - \frac{j_L A_s r_i^2}{2\kappa}\left[\frac{(r_e/r_i)^2 - 1}{2} - \ln\left(\frac{r_e}{r_i}\right)\right] = 0 \qquad (9)$$

where r_e and r_i are the external and internal radius of the three-dimensional electrode, ΔE is the range of potentials where the reaction takes place at limiting current density, j_L, and κ is the effective electrolyte conductivity, evaluated by the Bruggeman equation

$$\kappa = \kappa^0 \varepsilon^{3/2} \qquad (10)$$

being κ^0 the electrolyte conductivity. Thus, Eq. (9) gives 7 mm as the optimal value of the bed depth for the three-dimensional anode. In this calculation, it was taken 1.2 V for the potential range, 0.8 as the efficiency factor of the specific surface area and 2.58 S m^{-1} for the conductivity, which was experimentally measured. The limiting current density was 4.7 mA cm^{-2}, according to the experimental results obtained with the bi-dimensional rotating cylinder electrode reported on Fig. 6.

Fig. 9 displays the figures of merit for the production of colloidal sulphur as a function of the anodic potential when three-dimensional anodes of different bed thicknesses are used. A bed depth of 8 mm appears as the best option because it shows a space time yield only slightly smaller than that of the thicker electrode with specific energy consumption similar to the thinner one, showing a high current efficiency. The space time yield for 8 mm as bed depth is 2.0 kg m^{-3} h^{-1}, in the potential range of 0.8 V to 1.2 V, 5 times higher than those of the bi-dimensional electrode, with a specific energy consumption of 11.7 kW h kg^{-1}. It must be emphasised that the optimal bed depth, experimentally determined, agrees quite well with that theoretically predicted by Eq. (9).

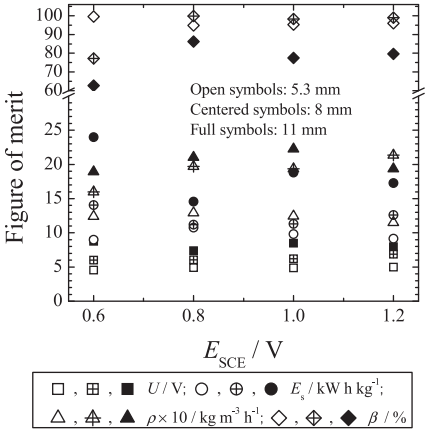

Fig. 9. Figures of merit for the colloidal sulphur production at three-dimensional rotating cylinder electrodes coated with lead as a function of the anodic potential for different bed depths. Electrolyte: 2 g S$^=$ dm^{-3}, pH 10. T = 80 °C. ω = 500 rpm.

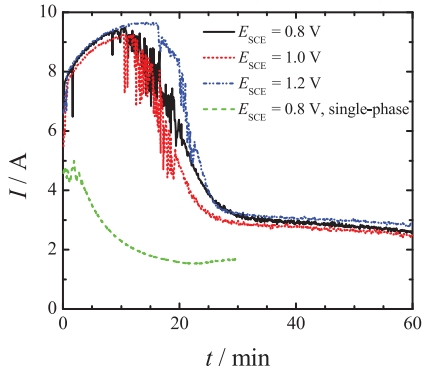

Fig. 10. Current as a function of time for sulphide oxidation at a three-dimensional rotating cylinder electrode coated with lead in a biphasic system. Bed depth: 8 mm. Electrolyte: 2 g S$^=$ dm^{-3}, initial pH ≅ 14. T = 80 °C. ω = 500 rpm. Gas volumetric flow rate: 8 × 10^{-6} m^3 s^{-1}.

Fig. 10 reports on the current as a function of time for a three-dimensional rotating cylinder electrode, bed depth 8 mm, working in the biphasic electrolyte. As comparison the curve for the single-phase system is also shown, revealing that in both cases the same general behaviour is observed. The stationary value of current is higher in the biphasic system probably due to the presence of the gas stream replenishes sulphide ions in the solution by dissolution of the hydrogen sulphide. Taking into account the mass of sulphur produced and the final sulphide concentration it can be expected the formation of S_2^{2-} in the single phase experiments and S_5^{2-} in the biphasic system.

Fig. 11 compares the figures of merit for the single-phase and biphasic system as a function of potential. The further increase of the space time yield to a value of 3.6 kg m^{-3} h^{-1} can be recognised as the main aspect of the biphasic system improving the reactor performance.

4. Mathematical modelling of the three-dimensional electrode in a biphasic system

The mass-balance for a batch reactor yields

$$\frac{dc}{dt} = -\frac{I\beta}{2FV} + \frac{F_n}{V}(y_i - y_o) \qquad (11)$$

here c is the concentration of the reactant, HS^-, F_n the gas molar flow rate, y_i and y_o the molar fraction of hydrogen sulphide in the

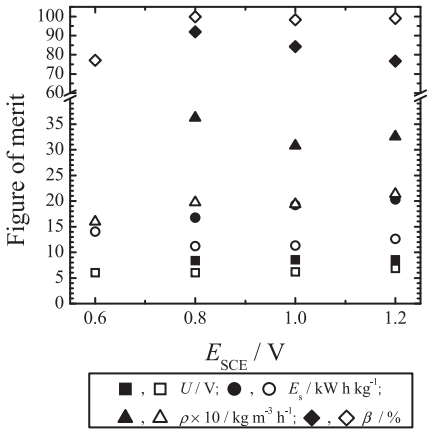

Fig. 11. Comparison of the figures of merit between single-phase and biphasic system for the colloidal sulphur production at a three-dimensional rotating cylinder electrode coated with lead as a function of the anodic potential. Bed depth: 8 mm. Electrolyte: 2 g S$^{=}$ dm^{-3}. T = 80 °C. ω = 500 rpm. Gas volumetric flow rate: 8×10^{-6} m^3 s^{-1}. Full symbols: biphasic system at initial pH ≅ 14. Open symbols: single-phase electrolyte.

gas phase at the inlet and outlet of the reactor, respectively. The first term on the right hand side in Eq. (11) represents the electrochemical reaction and the absorption of hydrogen sulphide in the reactor is given by the second one.

A mass-balance in the gas phase inside the three-dimensional structure as a function of the radial position, r, gives

$$\frac{dy}{dr} = -\frac{kA_aP2\pi Lr}{HF_n}\left(y - \frac{c}{A}\right) \tag{12}$$

where the product between the overall mass-transfer coefficient, k, and the specific surface area in the gas-liquid interface, A_a, is given by

$$\frac{1}{kA_a} = \frac{1}{k_gA_a/H} + \frac{1}{k_lA_a} \tag{13}$$

and

$$A = \frac{K_1P}{Hc_H} \tag{14}$$

being k_g and k_l the gas-side and liquid-side mass-transfer coefficients at the gas-liquid interface, respectively, K_1 the first dissociation constant of hydrogen sulphide, H the Henry's constant, c_H the concentration of the hydrogen ions in the solution, P the total pressure and L the height of the electrode. In engineering calculations A_a cannot be accurately determined. For this reason the mass-transfer rates are reported in terms of transfer coefficients based on a unit electrode volume, $k\,A_a$, rather than on a unit of interfacial area, k. The integration of Eq. (12) results in

$$y_i - y_o = \left(y_i - \frac{c}{A}\right)\alpha \tag{15}$$

where

$$\alpha = 1 - \exp\left[-\frac{kA_aP\pi L}{HF_n}(r_e^2 - r_i^2)\right] \tag{16}$$

Introducing Eq. (15) into Eq. (11) and considering that the current becomes independent on time after a short transient period of few minutes, it is obtained

$$c(t) = A\left(y_i - \frac{I\beta}{2FF_n\alpha}\right) - \left[A\left(y_i - \frac{I\beta}{2FF_n\alpha}\right) - c(0)\right]\exp\left(-\frac{F_n\alpha}{VA}t\right) \tag{17}$$

Table 1
Physicochemical properties of the biphasic system.

System	Liquid phase ≅ 2 g S$^{=}$ dm^{-3} Gas phase ≅ 5% H_2S in N_2
K_1 (80 °C)/mol m^{-3} [45]	3.05×10^{-4}
H (80 °C)/atm m^3 mol^{-1} [46]	3.15×10^{-2}

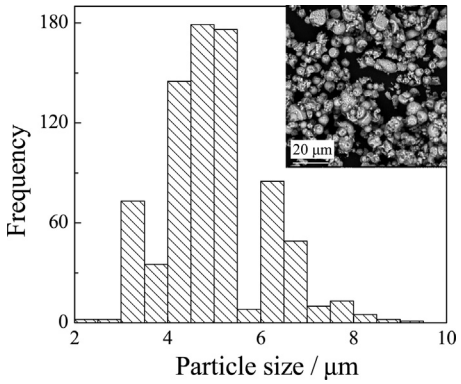

Fig. 12. Distribution of particle size in a sample of colloidal sulphur obtained with the biphasic electrolyte. ω = 500 rpm, E_{SCE} = 1.2 V. T = 80 °C. Inset: Scanning electron micrograph of colloidal sulphur. Magnification: ×3000.

Eq. (17) assumes that the absorption of hydrogen sulphide takes place mainly inside the three-dimensional structure and it is immediately transformed in HS^- which reacts at the electrode according to Eq. (3). Due to the high value of the constant A the argument of the exponential function in Eq. (17) is small and this function can be approximated by the two first term of a MacLaurin's series. Taking into account Eq. (6) results in

$$c(t) = c(0) - \frac{m(t)}{MV} - \left[\frac{c(0)}{A} - y_i\right]\frac{F_n\alpha}{V}t \tag{18}$$

Combining Eq. (18) with Eq. (16) the overall mass-transfer coefficient is given by

$$kA_a = -\frac{HF_n}{P\pi L(r_e^2 - r_i^2)}\ln\left\{1 - \frac{\left[c(t) - c(0) + \frac{m(t)}{MV}\right]V}{\left[y_i - \frac{c(0)}{A}\right]F_nt}\right\} \tag{19}$$

Table 1 displays the physicochemical parameters used in the calculations of the biphasic system. The computed kA_a value was 0.28 s^{-1} independent on the gas volumetric flow rate. This value is similar to those of the best gas-liquid absorbers reported by Charpentier [44], evidencing the good performance of a three-dimensional rotating cylinder electrode to carry out electrochemical reactions with gaseous reactants.

5. Morphological characterization of colloidal sulphur

A drop of the suspension of sulphur particles obtained at E_{SCE} = 1.2 V, vs. SCE, in the biphasic electrolyte was placed on a glass slide and allowed to dry. The supporting electrolyte was extracted by adding a drop of distilled water and absorbing the solution with filter paper. This procedure was repeated four times. The residual sulphur powder was dried in a desiccator over silica gel and the size of the particles and the surface morphology were examined by scanning electron microscopy. Fig. 12 shows the histogram of the particles, where it can be observed that the particle size is in the range of 2 μm to 9 μm with a mean value of 5 μm and a standard deviation of 1.09 μm. The statistical analysis is based on a sample of 785 independent measurements of the particle size. The sulphur powder presents different shapes with predominance of

spheroidal particles, as shown in the inset of Fig. 12. The EDS study of this sample revealed that sulphur was the only element in the powder, thus verifying the high purity of colloidal particles.

6. Conclusions

- Lead as anode material shows a good behaviour for the oxidation of sulphides in alkaline solutions at 80 °C in order to produce colloidal sulphur.
- A wide range of potentials of approximately 1.2 V is detected where the oxidation of sulphides to polysulphides takes place at a constant current density when the rotation rate is higher than 100 rpm. Under these mass-transfer conditions, probably a chemical intermediate is limiting the reaction rate.
- A batch electrochemical reactor with a rotating cylinder anode coated with lead exhibited a good performance for the electrosynthesis of polysulphides and the production of colloidal sulphur. The anodic and cathodic compartments must be separated by a cationic exchange membrane in order to avoid the reduction of polysulphide at the cathode.
- The use of an anode made with a three-dimensional structure, coated with lead, allowed to increase 5 times the space time yield of the reactor. Likewise, the replenishment of the sulphide ions by dissolution of hydrogen sulphide from a gas stream produces a further increase in this figure of merit to 3.6 $kg\,m^{-3}\,h^{-1}$.
- The optimal bed depth experimentally obtained, 8 mm, agrees satisfactorily with the theoretical value given by a model of potential distribution in three-dimensional electrodes.

Acknowledgements

This work was supported by the Agencia Nacional de Promoción Científica y Tecnológica (ANPCyT), Consejo Nacional de Investigaciones Científicas y Técnicas (CONICET) and Universidad Nacional del Litoral (UNL) of Argentina.

References

[1] J. Zaman, A. Chakma, Production of hydrogen and sulfur from hydrogen sulfide, Fuel Process. Technol. 41 (1995) 159.
[2] J.S. Eow, Recovery of sulfur from sour acid gas: A review of the technology, Environ. Prog. 21 (2002) 143.
[3] G.H. Kelsall, Electrochemical removal of H_2S, in: G. Kreysa, K.-i. Ota, R.F. Savinell (Eds.), Encyclopedia of Applied Electrochemistry, Springer, New York, 2014 p. 593.
[4] W.R. Fetzer, The electrolysis of sodium sulphide solutions, J. Phys. Chem. 32 (1928) 1787.
[5] G. Rajalo, T. Petrovskaya, Selective electrochemical oxidation of sulphides in tannery wastewater, Environ. Technol. 17 (1996) 605.
[6] G. Rajalo, T. Petrovskaya, V. Ahelik, Electrochemical oxidation of sulphide and thiosulphate ions using a hydrocyclone electrolytic cell, Proc. Estonian Acad. Sci. Chem. 46 (1997) 122.
[7] K. Waterston, D. Bejan, N. Bunce, Electrochemical oxidation of sulfide ion at a boron-doped diamond anode, J. Appl. Electrochem. 37 (2007) 367.
[8] M. Behm, D. Simonsson, Electrochemical production of polysulfides and sodium hydroxide from white liquor: Part I: Experiments with rotating disc and ring-disc electrodes, J. Appl. Electrochem. 27 (1997) 507.
[9] M. Behm, D. Simonsson, Electrochemical production of polysulfides and sodium hydroxide from white liquor: Part II: Electrolysis in a laboratory scale flow cell, J. Appl. Electrochem. 27 (1997) 519.
[10] M. Behm, D. Simonsson, Nickel as anode material for the electrochemical production of polysulfides in white liquor, J. New Mater. Electrochem. Syst. 2 (1999) 11.
[11] M. Behm, D. Simonsson, Graphite as anode material for the electrochemical production of polysulfide ions in white liquor, J. Appl. Electrochem. 29 (1999) 521.
[12] A.A. Anani, Z. Mao, R.E. White, S. Srinivasan, A.J. Appleby, Electrochemical production of hydrogen and sulfur by low temperature decomposition of hydrogen sulfide in an aqueous alkaline solution, J. Electrochem. Soc. 137 (1990) 2703.
[13] Z. Mao, A. Anani, R.E. White, S. Srinivasan, A.J. Appleby, A modified electrochemical process for the decomposition of hydrogen sulfide in an aqueous alkaline solution, J. Electrochem. Soc. 138 (1991) 1299.
[14] K. Petrov, S. Srinivasan, Low temperature removal of hydrogen sulfide from sour gas and its utilization for hydrogen and sulfur production, Int. J. Hydrogen Energy 21 (1996) 163.
[15] P. Lessner, F. McLarnon, J. Winnick, E. Cairns, Aqueous polysulphide flow-through electrodes: effects of electrocatalyst and electrolyte composition on performance, J. Appl. Electrochem. 22 (1992) 927.
[16] G.J.W. Radford, J. Cox, R.G.A. Wills, F.C. Walsh, Electrochemical characterisation of activated carbon particles used in redox flow battery electrode, J. Power Sources 185 (2008) 1499.
[17] P. Leung, X. Li, C. Ponce de León, L. Berlouis, C.T.J. Low, F.C. Walsh, Progress in redox flow batteries, remaining challenges and their applications in energy storage, RSC Advances 2 (2012) 10125.
[18] B. Dandapani, B.R. Scharifker, J.O.M. Bockris, Advancing toward technology breakout in energy conversion, A Symp. of the 21st Intersociety Energy Conversion Engineering Conf. 1 (1986) 262.
[19] Y.S. Shih, J.L. Lee, Continuous solvent extraction of sulfur from the electrochemical oxidation of a basic sulfide solution in the CSTER system, Ind. Eng. Chem. Process Des. Dev. 25 (1986) 834.
[20] Y. Qing-feng, C. Qi-yuan, Z. Ping-min, Electrochemical study of sulfide solution in the presence of surfactants, J. Environ. Sci. 10 (1998) 372.
[21] P.K. Dutta, R.A. Rozendal, Z. Yuan, K. Rabaey, J. Keller, Electrochemical regeneration of sulfur loaded electrodes, Electrochem. Commun. 11 (2009) 1437.
[22] Z. Lu, J. Tang, M. de Lourdes Mendoza, D. Chang, L. Cai, L. Zhang, Electrochemical decrease of sulfide in sewage by pulsed power supply, J. Electroanal. Chem. 745 (2015) 37.
[23] M. Farooque, T.Z. Fahidy, Low potential oxidation of hydrogen sulfide on a rotating tripolar wiper-blade electrode via continuous anode reactivation, J. Electrochem. Soc. 124 (1977) 1191.
[24] D.W. Kalina, E.T. Maas Jr., Indirect hydrogen sulfide conversion—I. An acidic electrochemical process, Int. J. Hydrogen Energy 10 (1985) 157.
[25] D.W. Kalina, E.T. Maas Jr., Indirect hydrogen sulfide conversion—II. A basic electrochemical process, Int. J. Hydrogen Energy 10 (1985) 163.
[26] K. Chandrasekara Pillai, T. Raju, S.J. Chung, I.-S. Moon, Removal of H_2S using a new Ce(IV) redox mediator by a mediated electrochemical oxidation process, J. Chem. Technol. Biotechnol. 84 (2009) 447.
[27] P.K. Dutta, K. Rabaey, Z. Yuan, J. Keller, Spontaneous electrochemical removal of aqueous sulfide, Water Res. 42 (2008) 4965.
[28] H.S. Lim, J. Winnick, Electrochemical removal and concentration of hydrogen sulfide from coal gas, J. Electrochem. Soc. 131 (1984) 562.
[29] B.G. Ateya, F.M. Al-Kharafi, Anodic oxidation of sulfide ions from chloride brines, Electrochem. Commun. 4 (2002) 231.
[30] B.G. Ateya, F.M. Al-Kharafi, R.M. Abdallah, A.S. Al-Azab, Electrochemical removal of hydrogen sulfide from polluted brines using porous flow through electrodes, J. Appl. Electrochem. 35 (2005) 297.
[31] D.R. Gabe, G.D. Wilcox, J. González-García, F.C. Walsh, The rotating cylinder electrode: its continued development and application, J. Appl. Electrochem. 28 (1998) 759.
[32] C.T.J. Low, C. Ponce de León, F.C. Walsh, The rotating cylinder electrode (RCE) and its application to the electrodeposition of metals, Aust. J. Chem. 58 (2005) 246.
[33] F.C. Walsh, G. Kear, A. Nahlé, J. Wharton, L. Arenas, The rotating cylinder electrode for studies of corrosion engineering and protection of metals—An illustrated review, Corros. Sci. (2017), doi:http://dx.doi.org/10.1016/j.corsci.2017.03.024.
[34] I. Hamilton, R. Woods, An investigation of the deposition and reactions of sulphur on gold electrodes, J. Appl. Electrochem. 13 (1983) 783.
[35] B. Scharifker, Z. Ferreira, J. Mozota, Electrodeposition of lead sulphide, Electrochim. Acta 30 (1985) 677.
[36] H.J. Wiesner, Lead, in: F.A. Lowenheim (Ed.), Modern Electroplating, John Wiley, New York, 1974 p. 266.
[37] M. King, Lead, in: R.E. Kirk, D.F. Othmer (Eds.), Encyclopedia of Chemical Technology, Wiley – Interscience, New York, 1998 p. 50.
[38] J.M. Bisang, Theoretical and experimental studies of the effect of side reactions in copper deposition from dilute solutions on packed-bed electrodes, J. Appl. Electrochem. 26 (1996) 135.
[39] W.E. Kleinjan, A.D. Keizer, A.J.H. Janssen, Kinetics of the chemical oxidation of polysulfide anions in aqueous solution, Water Res. 39 (2005) 4093.
[40] I.M. Kolthoff, E.B. Sandell, E.J. Meehan, S. Bruckenstein, Quantitative Chemical Analysis, 4th ed., Macmillan, London, 1969.
[41] H.E. Morris, R.E. Lacombe, W.H. Lane, Quantitative determination of elemental sulfur in aromatic hydrocarbons, Anal. Chem. 20 (1948) 1037.
[42] R. Alkire, B. Gracon, Flow-through porous electrodes, J. Electrochem. Soc. 122 (1975) 1594.
[43] G. Kreysa, K. Jüttner, J.M. Bisang, Cylindrical three-dimensional electrodes under limiting current conditions, J. Appl. Electrochem. 23 (1993) 707.
[44] J.-C. Charpentier, Mass-transfer rates in gas-liquid absorbers and reactors, in: T.B. Drew, G.R. Cokelet, J.W. Hopes, T. Vermeulen (Eds.), Advances in Chemical Engineering, 11, Academic Press, New York, 1981 pp .1.
[45] J.P. Hershey, T. Plese, F.J. Millero, The pK1* for the dissociation of H_2S in various ionic media, Geochim. Cosmochim. Acta 52 (1988) 2047.
[46] J.J. Carroll, A.E. Mather, The solubility of hydrogen sulphide in water from 0 to 90 °C and pressures to 1 MPa, Geochim. Cosmochim. Acta 53 (1989) 1163.